01 Jan 2005

Adaptive Critic Designs for Optimal Control of Power Systems

Ganesh K. Venayagamoorthy
Missouri University of Science and Technology

Ronald G. Harley

Recommended Citation

G. K. Venayagamoorthy and R. G. Harley, "Adaptive Critic Designs for Optimal Control of Power Systems," *Proceedings of the 13th International Conference on, Intelligent Systems Application to Power Systems, 2005*, Institute of Electrical and Electronics Engineers (IEEE), Jan 2005.
The definitive version is available at https://doi.org/10.1109/ISAP.2005.1599253

Adaptive Critic Designs for Optimal Control of Power Systems

G. K. Venayagamoorthy, *Senior Member, IEEE*, and R. G. Harley, *Fellow, IEEE*

***Abstract*--The increasing complexity of the modern power grid highlights the need for advanced modeling and control techniques for effective control of excitation, turbine and Flexible AC Transmission Systems (FACTS). The crucial factors affecting the modern power systems today is voltage and load flow control. Simulation studies in the PSCAD/EMTDC environment and real-time laboratory experimental studies carried out are described and the results show the successful control of the power system elements and the entire power system with adaptive and optimal neurocontrol schemes. Performances of the neurocontrollers are compared with the conventional PI controllers for damping under different operating conditions for small and large disturbances.**

***Index Terms*—Approximate Dynamic Programming, Reinforcement Learning, Optimal Control, Neural Networks, Excitation Control, Turbine Control, SSSC, SCRC, FACTS Devices.**

I. Introduction

POWER system control essentially requires a continuous balance between electrical power generation and a varying load demand, while maintaining system frequency, voltage levels and the power grid security. However, generator and grid disturbances can vary between minor and large imbalances in mechanical and electrical generated power, while the characteristics of a power system change significantly between heavy and light loading conditions, with varying numbers of generator units and transmission lines in operation at different times. The result is a highly complex and non-linear dynamic electric power grid with many operational levels made up of a wide range of energy sources with many interaction points. As the demand for electric power grows closer to the available sources, the complex systems that ensure the stability and security of the power grid are pushed closer to their edge. Thus, the need for advanced modeling and control techniques for the effective control of power system elements.

Adaptive critic designs (ACDs) are neural network designs capable of optimization over time, under conditions of noise and uncertainty. This family of ACDs brings new optimization techniques which combine concepts of reinforcement learning and approximate dynamic programming, thus making them powerful tools. The adaptive critic method provides a methodology for designing optimal nonlinear controllers using neural networks for complex systems such as the power system where accurate models are difficult to derive.

This paper describes the work of the authors based on adaptive critics for designing excitation and turbine neurocontrollers for generators [1]-[3] and FACTS devices (SSSCs and SCRCs) [4], [5] which overcome the risk of instability [6], the problem of residual error in the system identification [7], input uncertainties [8], and the computational load of online training. The neurocontroller augments/replaces the conventional PI controllers, and is trained in an offline mode prior to commissioning. Two different types of Adaptive Critics are discussed, namely the Heuristic Dynamic Programming (HDP) type and the Dual Heuristic Programming (DHP) type. Results are presented for a single-machine-infinite-bus, as well as for a multimachine power system with and without FACTS devices.

II. Adaptive Critic Designs

A. Background

The simplest adaptive critic designs learn slowly on large problems but they are successful on many real world difficult small problems. Complex adaptive critics may seem breathtaking, at first, but they are the only design approach that shows potential of replicating critical aspects of human intelligence: ability to cope with a large number of variables in parallel, in real time, in a noisy nonlinear non-stationary environment.

A family of ACDs was proposed by Werbos [9] as a new optimization technique combining concepts of reinforcement learning and approximate dynamic programming. For a given series of control actions that must be taken sequentially, and not knowing the effect of these actions until the end of the sequence, it is impossible to design an optimal controller using the traditional supervised learning neural network. The adaptive critic method determines optimal control laws for a system by successively adapting two ANNs, namely an ***action neural network*** (which dispenses the control signals) and a ***critic neural network*** (which 'learns' the desired performance index for some function associated with the performance index). These two neural networks approximate the Hamilton-Jacobi-Bellman equation associated with optimal control theory. The adaptation process starts with a non-optimal,

The support from the National Science Foundation under the grants - CAREER ECS # 0348221, ECS # 0400657, ECS # 0231632 and ECS # 0080764 is gratefully acknowledged by the authors.

G. K. Venayagamoorthy is with the Real-Time Power and Intelligent Systems (RTPIS) Laboratory, Department of Electrical and Computer Engineering, University of Missouri Rolla, MO 65409, USA (e-mail: gkumar@ieee.org).

R. G. Harley is with School of Electrical and Computer Engineering, Georgia Institute of Technology, Atlanta, GA 30332, USA (e-mail: ron.harley@ece.gatech.edu).

1-59975-028-7/05/$20.00 © 2005 ISAP.

arbitrarily chosen, control by the action network; the critic network then guides the action network towards the optimal solution at each successive adaptation. During the adaptations, neither of the networks need any 'information' of an optimal trajectory, only the desired cost needs to be known. Furthermore, this method determines optimal control policy for the entire range of initial conditions and needs no external training, unlike other neurocontrollers.

Dynamic programming prescribes a search which tracks backward from the final step, retaining in memory all suboptimal paths from any given point to the finish, until the starting point is reached. The result of this is that the procedure is too computationally expensive for most real problems. In supervised learning, an ANN training algorithm utilizes a desired output and, having compared it to the actual output, generates an error term to allow the network to learn. The backpropagation algorithm is typically used to obtain the necessary derivatives of the error term with respect to the training parameters and/or the inputs of the network. However, backpropagation can be linked to reinforcement learning via the critic network which has certain desirable attributes.

The technique of using a critic, removes the learning process one step from the control network (traditionally called the "action network" or "actor" in ACD literature), so the desired trajectory is not necessary. The critic network learns to approximate the ***cost-to-go*** or strategic utility function (the function J of Bellman's equation in dynamic programming) and uses the output of the action network as one of its inputs, directly or indirectly.

In the Dynamic Programming, or Markov Decision Process (MDP), Literature, problems are described in terms of five essential characteristics:

- Epochs
- States
- Actions
- Rewards
- Transition probabilities.

Most of the literature has focused on finite state spaces, where states are known with certainty. Actions may have probabilistic rules associated with them, and rewards and (obviously) transition probabilities may also be nondeterministic. Recent literature has addressed the extension to where states are also nondeterministic. These are known as Partially Observable Markov Decision Processes (POMDP's). It is straightforward to show that a POMDP can be transformed to a regular MDP with continuously-valued state variables. Since Adaptive Critics typically have been used in control problems with continuous-valued state spaces, they trivially are applicable to POMDP's. This observation, by itself, is sufficient reason for the family of Adaptive Critic approaches to be known and utilized outside the confines of the Intelligent Control community.

Different types of critics have been proposed. For example, Watkins [10] developed a system known as Q-learning, explicitly based on dynamic programming. Werbos, on the other hand, developed a family of systems for approximating dynamic programming [9]; his approach subsumes other designs for continuous domains. For example, Q-learning becomes a special case of Action-Dependent Heuristic Dynamic Programming (ADHDP), which is a critic approximating the J function (see section B below), in Werbos' family of adaptive critics. A critic which approximates only the derivatives of the function J with respect to its states, called the Dual Heuristic Programming (DHP), and a critic approximating both J and its derivatives, called the Globalized Dual Heuristic Programming (GDHP), complete this ACD family. These systems do not require exclusively neural network implementations, since any differentiable structure is suitable as a building block. The interrelationships between members of the ACD family have been generalized and explained in detail by Prokhorov [11, 12].

B. Heuristic Dynamic Programming

Fig. 1 shows a model dependent HDP Critic/Action design. The HDP Critic neural network is connected to the Action neural network through a Model neural network of the plant. These three different neural networks are each described in below and are taken for the purposes of this study to be a three-layer feedforward neural network with a single hidden layer with sigmoid transfer function. The input and output layers have linear transfer functions.

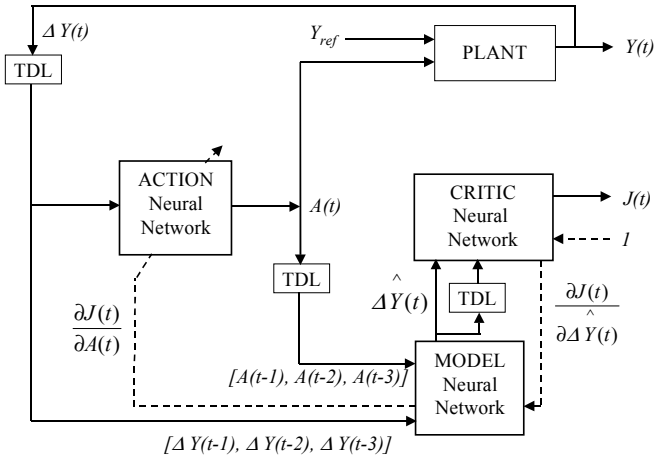

Fig. 1 A model dependent HDP critic/action design.

For model dependent designs it is assumed that there exists a Model neural network which is able to predict the states/outputs $Y(t+1)$, of the plant at time $t+1$, given at time t, the states/outputs $Y(t)$ and the action signals $A(t)$.

$$\hat{Y}(t+1) = f(Y(t), A(t)) \tag{1}$$

In addition to signals at time t, delayed values of these signals can be used as well depending of the complexity of the plant dynamics [13]. For the purposes of this study, the Model neural network predicts the *changes* in the outputs $\Delta Y(t+1)$, at time $t+1$ [13]. In Fig. 1, the inputs to the Model network are time-delayed values (TDL) of both the plant and the Action network outputs.

A neural network based technique to develop a Model network using supervised learning is shown in Fig. 2 and more

details can be found in [14]. The conventional static backpropagation algorithm is used in training the neural network. This Model neural network can undergo *offline* or *online* training, as required by the application.

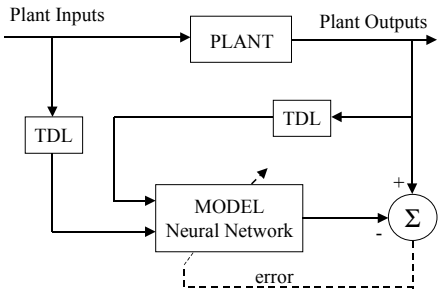

Fig. 2 Development of a neural network model of a plant.

Heuristic Dynamic Programming has a Critic neural network that estimates the function J (cost-to-go) in the Bellman equation of dynamic programming, expressed as follows:

$$J(Y(t)) = \sum_{k=0}^{\infty} \gamma^k U(Y(t+k)) \tag{2}$$

where γ is a discount factor for finite horizon problems ($0 < \gamma < 1$), $U(.)$ is the utility function or the local cost and $Y(t)$ is an input vector to the Critic. The Critic neural network is trained forward in time (multi-time steps ahead), which is of great importance for real-time operation.

Fig. 3 shows the HDP Critic adaptation/training. The inputs to the Critic are outputs from the Model neural network and its time-delayed values (Fig. 1). Two Critic neural networks are shown in Fig. 3 having the same inputs and outputs but at different time instants. The first Critic neural network has inputs from time steps t, $t-1$ and $t-2$, and the second Critic neural network has inputs from time steps $t+1$, t and $t-1$. Their corresponding outputs are $J(t)$ and $\hat{J}(t+1)$ respectively. The second Critic neural network estimates the function $\hat{J}$ (cost-to-go) at time $t+1$ by using the Model neural network to get inputs one step ahead. As a result it is possible to know the Critic neural network output $\hat{J}(t+1)$ at time t.

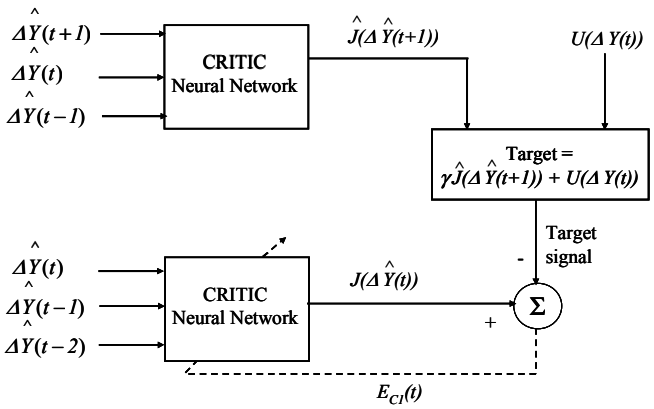

Fig. 3 HDP Critic neural network adaptation/training.

The Critic network tries to minimize the following error measure over time

$$\|E_1\| = \frac{1}{2}\sum_t E_{C1}^2(t) \tag{3}$$

$$E_{C1}(t) = \hat{J}(\Delta\hat{Y}(t)) - \gamma\hat{J}(\Delta\hat{Y}(t+1)) - U(\Delta Y(t)) \tag{4}$$

where $\Delta Y(t)$ is the changes in $Y(t)$, a vector of observables of the plant (or the states, if available). The utility function U is dependent on the system controlled and a typical function is given in [2]. It should be noted that only for the purposes of this study, changes in the state variables are used rather than state variables. The necessary condition for (2) to be minimal is given in (5).

$$\frac{1}{2}\frac{\partial}{\partial W_{C1}}\left\langle E_{C1}^2(t)\right\rangle = \left\langle E_{C1}\frac{\partial E_{C1}(t)}{\partial W_{C1}}\right\rangle = 0 \tag{5}$$

The weights' update for the Critic network using the backpropagation algorithm is given as follows:

$$\Delta W_{C1} = -\eta \quad E_{C1}(t)\frac{\partial E_{C1}(t)}{\partial W_{C1}} \tag{6}$$

$$\Delta W_{C1} = -\eta\{\hat{J}(\Delta\hat{Y}(t)) - \gamma\hat{J}(\Delta\hat{Y}(t+1)) - U(\Delta Y(t))\}\times \frac{\partial\{\hat{J}(\Delta\hat{Y}(t)) - \gamma\hat{J}(\Delta\hat{Y}(t+1)) - U(\Delta Y(t))\}}{\partial W_{C1}} \tag{7}$$

where η is a positive learning rate and W_{C1} are the weights of the Critic neural network. The same Critic network is shown in two consecutive moments in time in Fig. 3. The Critic network's output $\hat{J}(\Delta\hat{Y}(t+1))$ is necessary in order to provide the training signal $\gamma\hat{J}(\Delta\hat{Y}(t+1)) + U(\Delta Y(t))$, which is the desired/target value for $\hat{J}(\Delta\hat{Y}(t))$.

The objective of the Action neural network in Fig. 1, is to minimize *J(ΔY(t))* in the immediate future, thereby optimizing the overall cost expressed as a sum of all *U(ΔY (t))* over the horizon of the problem. This is achieved by training the Action neural network with an error signal *∂J/∂A*. The gradient of the cost function *J*, with respect to the outputs *A*, of the Action neural network, is obtained by backpropagating *∂J/∂J* (i.e. the constant *1*) through the Critic neural network and then through the pretrained Model neural network to the Action neural network. This gives *∂J/∂A* and *∂J/∂W_A* for all the outputs of the Action neural network, and all the Action neural network's weights *W_A*, respectively. The weights' update in the Action neural network using backpropagation algorithm is given as follows:

$$\|E_2\| = \frac{1}{2}\sum_t E_{A1}^2(t) \tag{8}$$

where

$$E_{A1} = \frac{\partial J(t)}{\partial A(t)} \tag{9}$$

and

$$\frac{\partial J(t)}{\partial A(t)} = \frac{\partial J(t)}{\partial \Delta \hat{Y}(t)} \frac{\partial \Delta \hat{Y}(t)}{\partial A(t)} \tag{10}$$

Weight change in the Action network ΔW_{A1} can be written as:

$$\Delta W_{A1} \propto \frac{\partial E_2}{\partial W_A} \tag{11}$$

Equation (11) can be further written as:

$$\Delta W_{A1} = -\alpha E_{A1}(t) \frac{\partial E_{A1}(t)}{\partial W_{A1}} \tag{12}$$

$$\Delta W_{A1} = -\alpha \frac{\partial J(t)}{\partial A(t)} \frac{\partial}{\partial W_{A1}} \left(\frac{\partial J(t)}{\partial A(t)} \right) \tag{13}$$

where α is a positive learning rate.

With (7) and (13), the training of the Critic and the Action networks can be carried out. The general training procedure for the Critic and the Action networks are described in Section D.

C. Dual Heuristic Programming

The Critic neural network in the DHP scheme shown in Fig. 4, estimates the derivatives of *J* with respect to the vector $\hat{\Delta Y}$ (outputs of the Model neural network) and learns minimization of the following error measure over time:

$$\|E_3\| = \sum E_{C2}^T(t) E_{C2}(t) s \tag{14}$$

where

$$E_{C2}(t) = \frac{\partial J(\Delta \hat{Y}(t))}{\partial \Delta \hat{Y}(t)} - \gamma \frac{\partial \hat{J}(\Delta \hat{Y}(t+1))}{\partial \Delta Y(t)} - \frac{\partial U(\Delta Y(t))}{\partial \Delta Y(t)} \tag{15}$$

where *∂(.)/∂ΔY(t))* is a vector containing partial derivatives of the scalar (.) with respect to the components of the vector *ΔY*. The Critic neural network's training is more complicated than in HDP, since there is a need to take into account all relevant pathways of backpropagation as shown in Fig. 4, where the paths of derivatives and adaptation of the Critic are depicted by dashed lines. In Fig. 4, the dashed lines mean the first backpropagation and the dotted-dashed lines mean the second backpropagation.

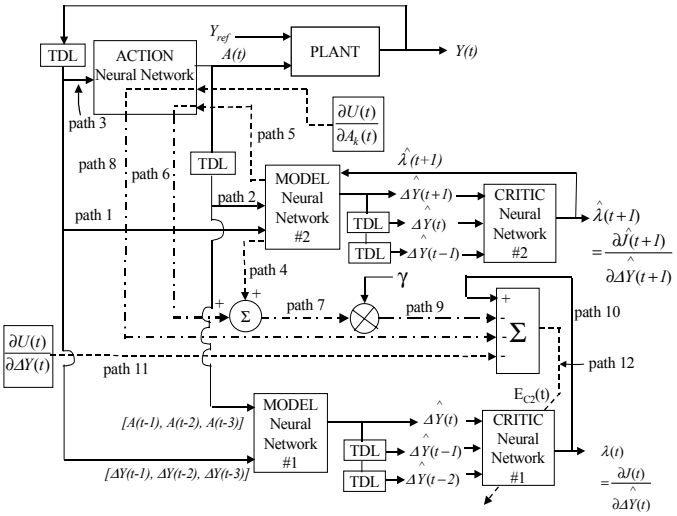

Fig. 4 DHP Critic neural network adaptation.

The Model neural network in the design of DHP Critic and Action neural networks are obtained in a similar manner to that described in Section B above.

In the DHP scheme, application of the chain rule for derivatives yields:

$$\frac{\partial \hat{J}(\Delta \hat{Y}(t+1))}{\partial \Delta Y_j(t)} = \sum_{i=1}^{n} \hat{\lambda}_i(t+1) \frac{\partial \Delta \hat{Y}_i(t+1)}{\partial \Delta Y_j(t)} + \sum_{k=1}^{m}\sum_{i=1}^{n} \hat{\lambda}_i(t+1) \frac{\partial \Delta \hat{Y}_i(t+1)}{\partial A_k(t)} \frac{\partial A_k(t)}{\partial \Delta Y_j(t)} \tag{16}$$

where $\hat{\lambda}_i(t+1) = \partial \hat{J}(\Delta \hat{Y}(t+1)) \big/ \partial \Delta \hat{Y}_i(t+1)$, and *n*, *m*, *j* are the numbers of outputs of the Model, Action and Critic neural networks respectively. By exploiting (16), each of *n* components of the vector $E_{C2}(t)$ from (15) is determined by

$$E_{C2j}(t) = \frac{\partial J(\Delta \hat{Y}(t))}{\partial \Delta \hat{Y}_j(t)} - \gamma \frac{\partial \hat{J}(\Delta \hat{Y}(t+1))}{\partial \Delta Y_j(t)} - \frac{\partial U(\Delta Y(t))}{\partial \Delta Y_j(t)} - \sum_{k=1}^{m} \frac{\partial U(t)}{\partial A_k(t)} \frac{\partial A_k(t)}{\partial \Delta Y_j(t)} \quad (17)$$

The signals in Fig. 4 which are labeled with a path number, represent the following:

(i). Path 1 represents the outputs of the plant fed into the Model neural network #2. These outputs are *ΔY(t)*, *ΔY(t-1)* and *ΔY(t-2)*.

(ii). Path 2 represents the outputs of the Action neural network fed into the Model neural network #2. These outputs are *A(t)*, *A(t-1)* and *A(t-2)*.

(iii). Path 3 represents the outputs of the plant fed into the Action neural network. These outputs are *ΔY(t)*, *ΔY(t-1)* and *ΔY(t-2)*.

(iv). Path 4 represents a backpropagated signal of the output of the Critic neural network #2 through the Model neural network with respect to path 1 inputs. The backpropagated signal on path 4 is $\sum_{i=1}^{n} \hat{\lambda}_i(t+1) \frac{\partial \Delta \hat{Y}_i(t+1)}{\partial \Delta Y_j(t)}$ in (16).

(v). Path 5 represents a backpropagated signal of the output of the Critic neural network #2 through the Model neural network with respect to path 2 inputs. The backpropagated signal on path 3 is $\sum_{i=1}^{n} \hat{\lambda}_i(t+1) \frac{\partial \Delta \hat{Y}_i(t+1)}{\partial A_k(t)}$ in (16).

(vi). Path 6 represents a backpropagation output of path 5 signal ((iv) above) with respect to path 3. The signal on path 6 is $\sum_{k=1}^{m} \sum_{i=1}^{n} \hat{\lambda}_i(t+1) \frac{\partial \Delta \hat{Y}_i(t+1)}{\partial A_k(t)}$ in (16).

(vii). Path 7 is the sum of the path 4 and path 6 signals resulting in $\partial \hat{J}(\Delta \hat{Y}(t+1)) \big/ \partial \Delta Y_j(t)$, given in (16).

(viii). Path 8 is the backpropagated signal of the term $\partial U(t)/\partial A_k(t)$ (Fig. 5) with respect to path 3 and is $\sum_{k=1}^{m} \frac{\partial U(t)}{\partial A_k(t)} \frac{\partial A_k(t)}{\partial \Delta Y_j(t)}$ in (17).

(ix). Path 9 is a product of the discount factor γ and the path 7 signal, resulting in term $\gamma \partial \hat{J}(\Delta \hat{Y}(t+1)) \big/ \partial \Delta Y_j(t)$ in (17).

(x). Path 10 represents the output of the Critic neural network #1, $\partial J(\Delta \hat{Y}(t)) \big/ \partial \Delta \hat{Y}(t)$.

(xi). Path 11 represents the term $\partial U(t)/\partial \Delta Y(t)$ (Fig. 5).

(xii). Path 12 represents $E_{C2j}(t)$ given in (17) and as follows: *Path 12 = $E_{C2j}(t)$ = path 10 – path 9 – path 11 – path 8*.

The partial derivatives of the utility function *U(t)* with respect to $A_k(t)$, and $\Delta Y(t)$, $\partial U(t)/\partial A_k(t)$ and $\partial U(t)/\partial \Delta Y(t)$ respectively, are obtained by backpropagating the utility function, *U(t)* through the Model network as shown in Fig. 5.

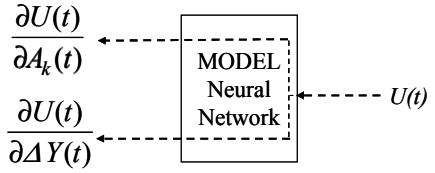

Fig. 5 Backpropagation of U(t) through the Model neural network.

The adaptation of the action network in Fig. 4, is illustrated in Fig. 6 which propagates $\lambda(t+1)$ back through the model network to the action network. The goal of such adaptation can be expressed as follows [11, 12]:

$$\frac{\partial U(\Delta Y(t))}{\partial A(t)} + \gamma \frac{\partial \hat{J}(\Delta \hat{Y}(t+1))}{\partial A(t)} = 0 \quad \forall \ t \quad (18)$$

The error signal for the Action network adaptation is therefore given as follows:

$$E_{A2}(t) = \frac{\partial U(\Delta Y(t))}{\partial A(t)} + \gamma \frac{\partial \hat{J}(\Delta \hat{Y}(t+1))}{\partial A(t)} \quad (19)$$

The weights' update expression [12], when applying backpropagation, is as follows:

$$\Delta W_{A2} = -\alpha \left[\frac{\partial U(\Delta Y(t))}{\partial A(t)} + \gamma \frac{\partial \hat{J}(\Delta \hat{Y}(t+1))}{\partial A(t)} \right]^T \frac{\partial A(t)}{\partial W_{A2}} \quad (20)$$

where α is a positive learning rate and W_{A2} are weights of the DHP Action neural network.

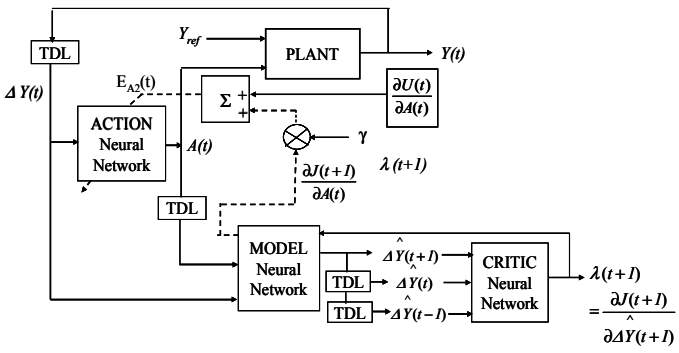

Fig. 6 DHP Action neural network adaptation.

D. General Training Procedure for the Critic and the Action Networks

The training procedure is that suggested in [12] and it is applicable to any ACD. It consists of two separate training cycles: one for the Critic, and the other for the Action. An important measure is that the Action neural network is pretrained with conventional controllers (Proportional Integral Derivative, PID) controlling the plant in a linear region. The

Critic's adaptation is done initially with the pretrained Action network, to ensure that the whole system, consisting of the ACD and the plant remains stable. Then the Action network is trained further while keeping the Critic neural network weights fixed. This process of training the Critic and the Action one after the other, is repeated until an acceptable performance is reached. It is assumed that there is no concurrent adaptation of the pretrained Model neural network, and W_C is initialized to small random values.

In the Critic's training cycle, an incremental optimization of (5) and/or (9) is carried out using a suitable optimization technique (e.g. backpropagation). The following operations are repeated N_C times:

1. Initialize $t = 0$ and $\Delta Y(0)$
2. Compute the output of the Critic neural network at time t, $J(t)$ or $\lambda(t) = f_C(\Delta Y(t), W_C)$
3. Compute the output of the Action neural network at time t, $A(t) = f_A(\Delta Y(t), W_A)$
4. Compute the output of the Model neural network at time $t+1$, $\Delta Y(t+1) = f_M(\Delta Y(t), A(t), W_M)$
5. Compute the output of the Critic neural network at time $t+1$, $\hat{J}(t+1)$ or $\hat{\lambda}(t+1) = f_C(\Delta Y(t+1), W_C)$
6. Compute the Critic neural network error at time t, $E_{C1}(t)$ from (5a) or $E_{C2}(t)$ from (10).
7. Update the Critic neural network's weights using the backpropagation algorithm.
8. Repeat steps 2 to 7.

The functions $f_C(\Delta Y(t), W_C)$, $f_A(\Delta Y(t), W_A)$ and $f_M(\Delta Y(t), A(t), W_M)$ represent the Critic, the Action and the Model neural networks with their weights W_i, respectively.

In the Action neural network's training cycle, an incremental learning is also carried out using the backpropagation algorithm, as in the Critic neural network's training cycle above, and the list of operations for the Action neural network's training cycle is almost the same as that for the Critic neural network's cycle above (steps 1 to 7). However, (7b) or (13) are used for updating the Action neural network's weights instead of using (5a) or (10). The Action's training cycle is repeated N_A times while keeping the Critic's weights W_C fixed. N_C and N_A are the lengths of the corresponding training cycles. It is important that the whole system consisting of the ACD and the plant remains stable while both of the Critic and Action networks undergo adaptation.

III. ACD Based Control Of Excitation And Turbine Systems Of Generators

The micro-machine laboratory at the University of Kwa-Zulu Natal, Durban, South Africa has two 3 kW, 220 V, three phase micro-alternators, and each one represents both the electrical and mechanical aspects of a typical 1000 MW alternator. The laboratory power system is simulated in the MATLAB/SIMULINK environment and simulations studies with neurocontrollers are carried out prior to hardware implementations. The laboratory single machine infinite bus power system in Fig. 7 consists of a micro-alternator, driven by a dc motor whose torque - speed characteristics are controlled by a power electronic converter to act as a micro-turbine, and a single short transmission line which links the micro-alternator to a voltage source which has a constant voltage and frequency, called an infinite bus. The parameters of the micro-alternators, determined by the IEEE standards are given in Tables I and II [15]. A time constant regulator is used to insert negative resistance in series with the field winding circuit [15], in order to reduce the actual field winding resistance to the correct per-unit value.

A three-machine power system shown in Fig. 8 is set up by using the two micro-alternators and the infinite bus as the third machine.

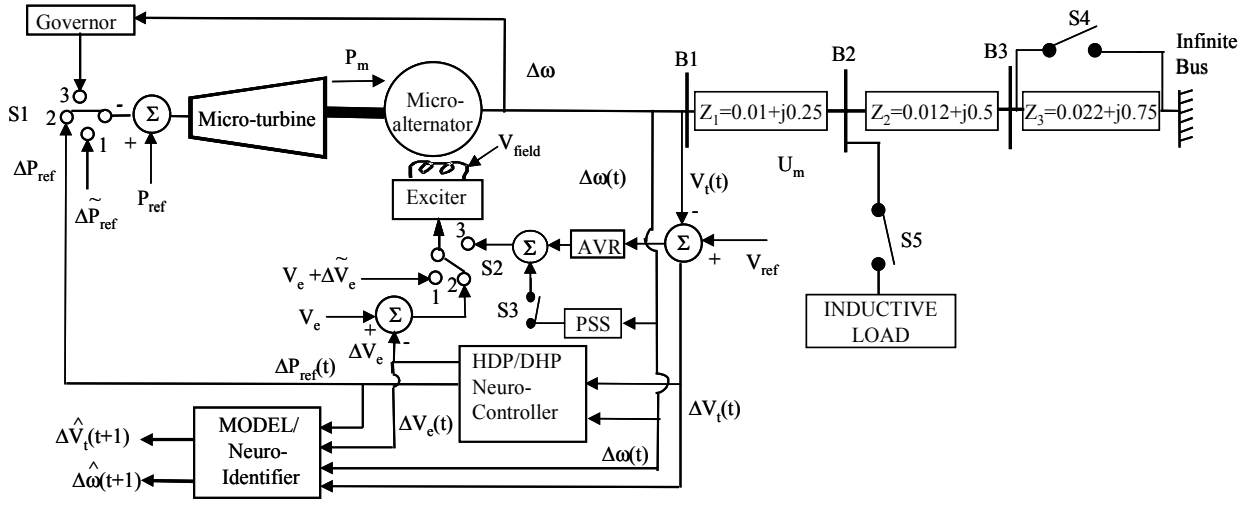

Fig. 7 The single machine infinite bus configuration with the conventional AVR and governor controllers, and neurocontroller.

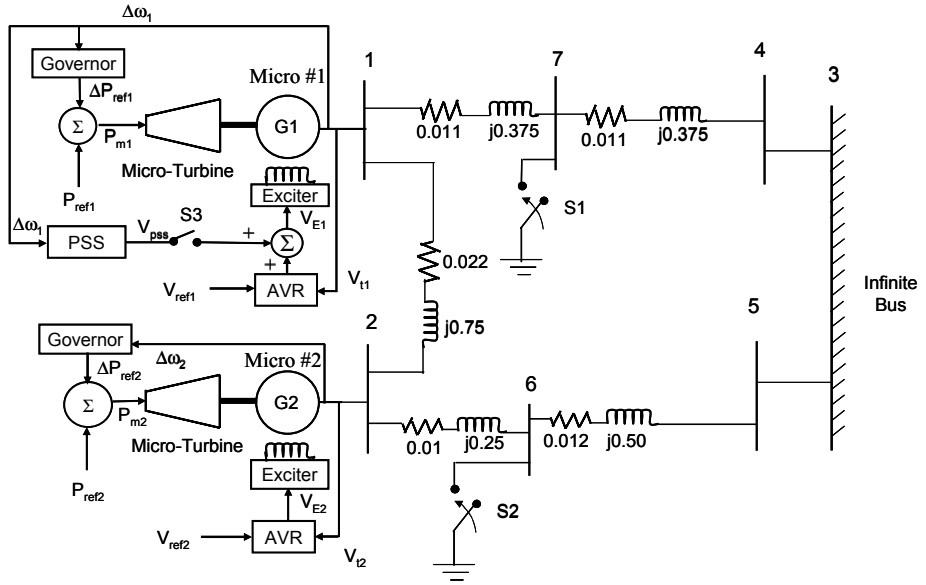

Fig. 8 Multimachine power system consisting of two micro-alternators G1 and G2 which are conventionally controlled by the AVRs, governors and a PSS.

A. Conventional Excitation and Turbine Control

The practical system uses a conventional AVR and exciter combination of which the transfer function block diagram is shown in Fig. 9, and the time constants and gain are given in Table III [15]. The exciter saturation factor S_e is given by

$$S_e = 0.6093 \exp(0.2165 V_{fd}) \tag{21}$$

T_{v1}, T_{v2}, T_{v3} and T_{v4} are the time constants of the PID voltage regulator compensator; T_{v5} is the input filter time constant; T_e is the exciter time constant; K_{av} is the AVR gain; V_{fdm} is the exciter ceiling voltage; and, V_{ma} and V_{mi} are the AVR maximum and minimum ceiling voltages.

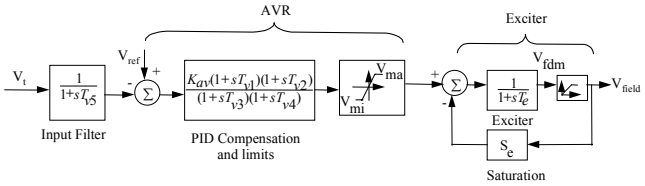

Fig. 9 Block diagram of the AVR and exciter combination.

The block diagram of the power system stabilizer (PSS) used to achieve damping of the system oscillations is shown in Fig. 10 [16]. The considerations and procedures used in the selection of the PSS parameters are similar to that found in [16] and these parameters are given in Table IV.

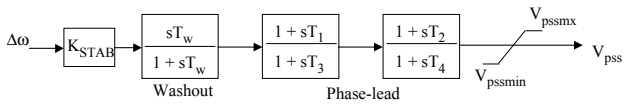

Fig. 10 Block diagram of the power system stabilizer.

A separately excited 5.6 kW thyristor controlled dc motor is used as a prime mover, called the micro-turbine, to drive the micro-alternator. The torque-speed characteristic of the dc motor is controlled to follow a family of rectangular hyperbola to emulate the different positions of a steam valve, as would occur in a real typical high pressure (HP) cylinder turbine. The three low pressure (LP) cylinders' inertia are represented by appropriately scaled flywheels attached to the micro-turbine shaft. The micro-turbine and governor combination transfer function block diagram is shown in Fig. 11, where, P_{ref} is the turbine input power set point value, P_m is the turbine output power, and $\Delta\omega$ is the speed deviation from the synchronous speed. The turbine and governor time constants and gain are given in Table V [15].

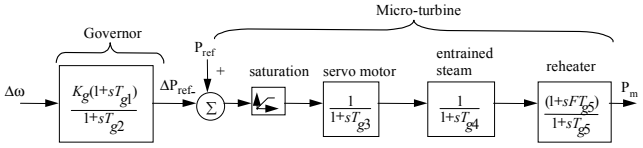

Fig. 11 Block diagram of the micro-turbine and governor combination.

The gains K_{av} (0.003) of the AVR and K_g (0.05) of the governor in Tables III and V respectively are obtained by suitable choices of the gain and phase margins in each case, as described in [17]. Transmission lines are represented by using banks of lumped inductors and capacitors.

B. Simulation and Experimental Studies with Different Control Schemes for Excitation and Turbine Systems

The dynamic and transient operation of the HDP and DHP neurocontrollers are compared with the operation of the conventional (CONV) controller (AVR and turbine governor, excluding the PSS) for single machine infinite bus power system in Fig. 7. In addition, the performance of a continually online trained neurocontroller (COT) is also shown. The COT neurocontroller is developed based on the indirect adaptive neurocontrol scheme [18]. In power systems faults such as three phase short circuits occur from time to time, and because they prevent energy from the generator reaching the infinite bus, it means that most of the turbine shaft power goes into

accelerating the generator during the fault. This represents a severe transient test for the controller performance. Figs. 12 and 13 show the response of all four controllers for the three phase temporary short circuit for 50 ms with the new transmission line impedance Z_2. Here, it is obvious that the DHP controller clearly beats the other three controllers in terms of offering the greatest oscillation damping especially in the rotor angle. The DHP controller proves its robustness to changes in the system configurations.

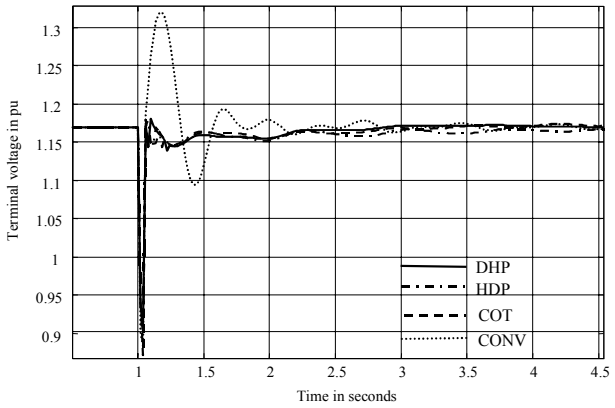

Fig. 12 Terminal voltage of the micro-alternator for a temporary 50 ms three phase short circuit (transmission line impedance Z_2).

Based on the results for the single machine power system in above, the DHP controller has the best performance, hence, the DHP neurocontroller is the only one that is now implemented on the multimachine power system. The performance of the DHP neurocontroller is now compared with that of the conventional controllers, one of which is equipped with a power system stabilizer. Fig. 14 shows the multimachine power system of Fig. 11 now equipped with two DHP neurocontrollers.

The DHP neurocontrollers were implemented on DSPs and allowed to control the laboratory multimachine power system [3]. The purpose of these tests is to confirm via practical measurements the potential of adaptive critic based neurocontrollers which have been demonstrated during the simulation studies for a single machine and a multimachine power system. However, the laboratory implementation on micro-machines is also intended to form a basis for possible future investigations into use of such neurocontrollers on large multi-megawatt sized power plants in a real-world power station.

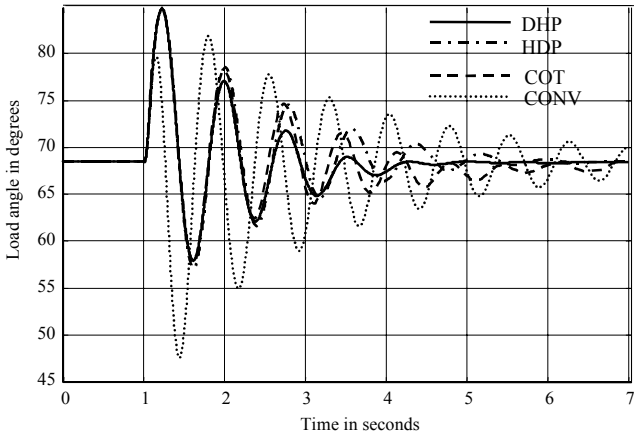

Fig. 13 Rotor angle of the micro-alternator for a temporary 50 ms three phase short circuit (transmission line impedance Z_2).

The DHP neurocontrollers are tested for dynamic and transient operation for an increase in the transmission line impedance by opening switch S2 in Figs. 11 and 14. Four different controller combination studies are carried out for the above disturbances and at different operating conditions for G1 and G2:

- Case a - conventional controller on both G1 and G2
- Case b - conventional controller with a PSS on G1 and conventional controller on G2
- Case c - DHP neurocontroller on G1 and conventional controller on G2
- Case d - DHP neurocontrollers on both G1 and G2.

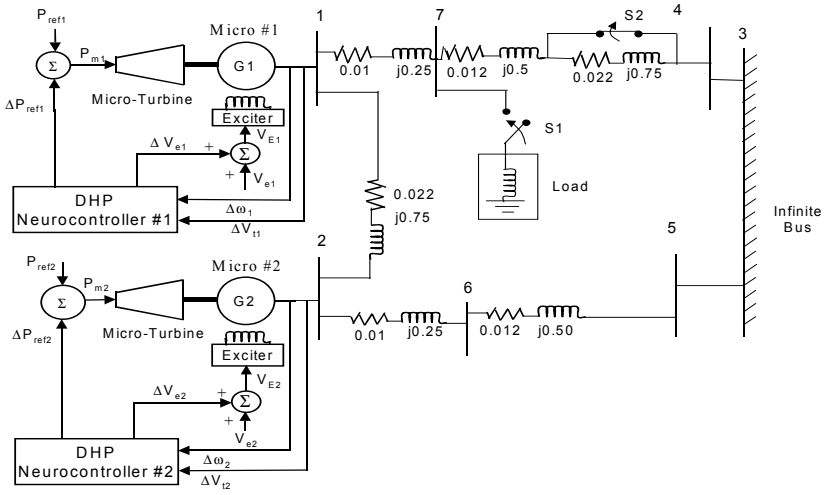

Fig. 14 Multimachine power system with two DHP neurocontrollers.

At the operating condition *(P = 0.2 pu, Q = 0 pu* on both generators*)*, the series transmission line impedance is increased at time t = 10 s from Z = 0.022 + j0.75 pu to Z = 0.044 + j1.50 pu by opening switch S2. Fig. 15 shows the load angle response of generator G2 for this test with the four different controller combinations. Clearly the DHP neurocontrollers (case d) again exhibit superior damping and ensure lesser overshoots compared to the performance of the conventional controllers even when equipped with a PSS. The load angle response of generator G1 for the same disturbance is shown in Fig.16. It is clear the DHP neurocontrollers exhibit the best damping of the controllers.

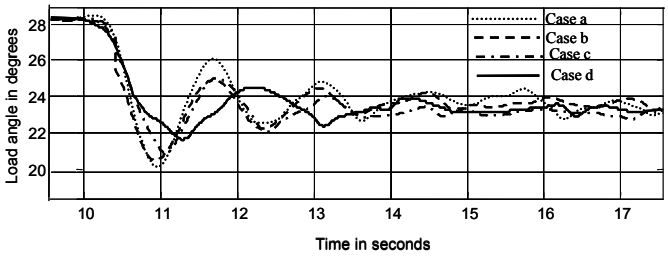

Fig. 15 Load angle response of generator G2 for series transmission line impedance increase by opening switch S2 for P = 0.2 pu and Q = 0 pu.

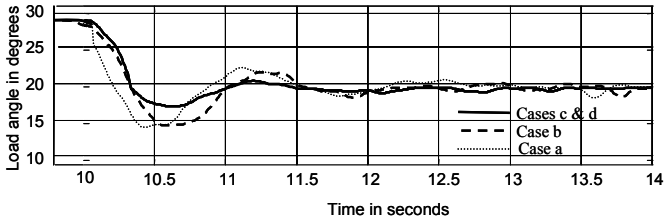

Fig. 16 Load angle response of generator G1 for series transmission line impedance increase by opening switch S2 for P = 0.2 pu and Q = 0 pu.

IV. ACD BASED CONTROL OF FACTS DEVICES

Currently, the control of FACTS devices are carried out using linear PI controllers with fixed parameters. The PI controller parameters are selected to give some desirable performance for a particular region of operation and conditions; outside which the performance of the controller degrades. Thus, the need for the design of a nonlinear robust/adaptive controller for FACTS devices arise to cater for a wide range of operating conditions and, to handle small and large disturbances.

The following subsections describe the SSSC and SCRC FACTS devices and the control schemes.

A. Static Synchronous Series Compensator (SSSC) and its Conventional Control Scheme

The static synchronous series compensator (SSSC) converter can control the reactive and/or active power on an ac system by changing both phasor angle and magnitude of the converter's output voltage with a fast control action. Especially, the exchange of active power, which is the particular characteristic of the SSSC, is accomplished by controlling the dc voltage inside the SSSC [19].

The single machine infinite bus (SMIB) system shown in Fig. 17 is used to compare the damping control capabilities of the Dual Heuristic Programming based neurocontroller (DHPNC) and the conventional PI controller (CONVC) for the SSSC. The plant consists of the synchronous generator (160 MVA, 15 kV (L-L)), turbine-governor system, automatic voltage regulator (AVR)-exciter system, transmission line connected to an infinite bus, and the SSSC connected in series with transmission line. The parameters of the synchronous generator and transmission line are given in [20].

The EXAC1A (IEEE alternator supplied rectifier excitation systems) and H_TUR1/GOV1 (IEEE type hydro turbine-governor) models in PSCAD/EMTDC software package are used as the AVR/exciter system and turbine/governor, respectively.

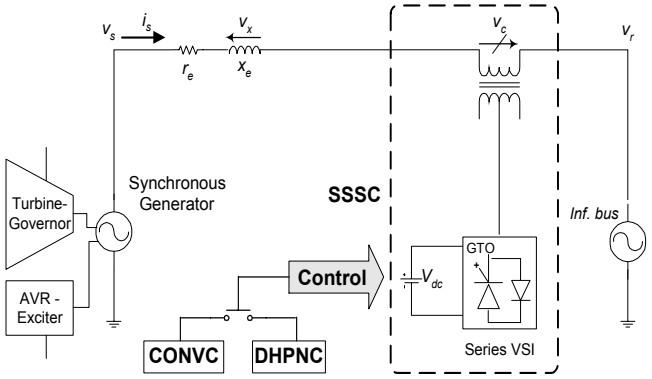

Fig. 17 Plant: 160 MVA, 15 kV (L-L) SMIB test system.

For the mathematical model of the SSSC, the associated equation can be represented with the lumped series transmission line reactance x'_e (transmission line x_e plus leakage reactance of series-connected transformer) and transmission series resistance r_e (the inverter is regarded simply to have no conduction losses) in per unit as follows.

$$\frac{d}{dt}\begin{bmatrix} i_{sa} \\ i_{sb} \\ i_{sc} \end{bmatrix} = \begin{bmatrix} -\frac{r_e\omega_s}{x'_e} & 0 & 0 \\ 0 & -\frac{r_e\omega_s}{x'_e} & 0 \\ 0 & 0 & -\frac{r_e\omega_s}{x'_e} \end{bmatrix} \begin{bmatrix} i_{sa} \\ i_{sb} \\ i_{sc} \end{bmatrix} + \begin{bmatrix} \frac{\omega_s}{x'_e}(v_{sa}+v_{ca}-v_{ra}) \\ \frac{\omega_s}{x'_e}(v_{sb}+v_{cb}-v_{rb}) \\ \frac{\omega_s}{x'_e}(v_{sc}+v_{cc}-v_{rc}) \end{bmatrix} \quad (22)$$

where ω_s is the synchronous speed of the power system, v_s is the sending-end voltage (terminal voltage in practice), i_s is the current in transmission line, v_r is the receiving-end voltage in the infinite bus, and v_c is the injected series compensation voltage.

Using the synchronously rotating reference frame based transformation [21] in which the d-axis is always coincident with the instantaneous voltage vector v and the q-axis leads the d-axis by 90°, the three-phase circuit equations in (22) can be transformed to the following d-q axis vector representation.

$$\frac{d}{dt}\begin{bmatrix} i_d \\ i_q \end{bmatrix} = \begin{bmatrix} -\frac{r_e\omega_s}{x'_e} & \omega \\ -\omega & -\frac{r_e\omega_s}{x'_e} \end{bmatrix} \begin{bmatrix} i_d \\ i_q \end{bmatrix} + \begin{bmatrix} \frac{\omega_s}{x'_e}(|v_s|+v_{cd}-v_{rd}) \\ \frac{\omega_s}{x'_e}(v_{cq}-v_{rq}) \end{bmatrix} \quad (23)$$

Neglecting the series inverter harmonics, the ac side injected voltage v_c in Fig. 12 can be expressed with relation to the capacitor voltage V_{dc} on the dc link as follows.

$$v_{cd} = mV_{dc}\cos(\alpha), \quad v_{cq} = mV_{dc}\sin(\alpha) \tag{24}$$

where α is the phase angle difference between the voltages v_c and v_s (the v_c leads the v_s), and m is the modulation index of the series inverter. The dynamics of the dc capacitor voltage are described by

$$\frac{dV_{dc}}{dt} = \frac{1}{C}\frac{P_{dc}}{V_{dc}} = \frac{1}{C}\frac{V_{dc}\,i_{dc}}{V_{dc}} = \frac{1}{C}\frac{(v_{cd}\,i_d + v_{cq}\,i_q)}{V_{dc}} = \frac{1}{C}\left[m\left\{\cos(\alpha)\,i_d + \sin(\alpha)\,i_q\right\}\right] \tag{25}$$

The main goal of the SSSC is to inject the series voltage in quadrature with the line current and to maintain the dc voltage V_{dc}. For this purpose, the *P-Q* (real and reactive power) automatic power flow control mode [19] in Fig. 18 is used.

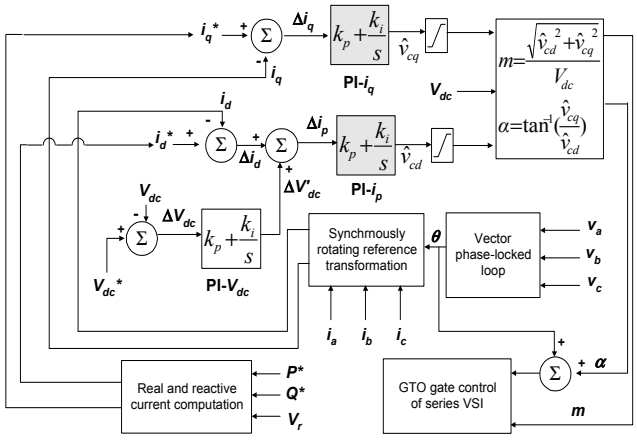

Fig. 18 *P-Q* automatic power flow control diagram for the internal control of the SSSC.

In Fig. 18, an instantaneous three-phase set of line voltages, v_a, v_b, and v_c is used to calculate the transformation angle, θ provided by the vector phase-locked loop for synchronous operation of the series voltage source inverter (VSI) shown in Fig. 17. As shown in (23), the three-phase set of measured line currents at the ac terminal of the SSSC is decomposed into its real/direct component, i_d, and reactive/quadrature component, i_q. These actual signals (i_d and i_q) and the reference d-q current signals (i_d^* and i_q^*) are compared, respectively.

The error signal Δi_q for the reactive power exchange is passed through the PI regulator PI-i_q. The signal Δi_p for the real power exchange and maintenance of a constant V_{dc}, is passed through the PI-i_p. The Δi_p consists of the Δi_d and error signal $\Delta V'_{dc}$ (which passes through the PI-V_{dc}). The V_{dc}^* is the desired value for V_{dc}. The value of V_{dc}^* is determined by selecting a suitable value of the modulation index within its range of 0 to 1.

B. Simulation Studies with Conventional and Neurocontrol for a Static Synchronous Series Compensator (SSSC)

To evaluate the damping performance of the proposed neurocontroller for the control of the SSSC, 100 ms and 120 ms three phase short circuits are applied *to the infinite bus* (receiving end) at t =1 s. The generator operates with a rotor angle of 53.6° (P_t=1.0 pu, Q_t= 0.59 pu) in a steady-state operating point. The results are shown in Figs. 19 to 21, where "Uncompensated" and "CONVC" denote the response of generator controlled without SSSC and with a PI controlled SSSC, respectively.

From the Figs. 19 and 20, the DHPNC damping control is more effective compared to the CONVC. Also, it is clear from Fig. 21 that the generator controlled without the SSSC goes unstable and loses synchronism when the fault duration is 120 ms. In contrast, the DHPNC and CONVC restore the generator to a stable mode, and the DHPNC damping control is more effective compared to the CONVC, which means that the DHPNC allows the generator to be operated closer to its stability limit. Detailed results and explanations are given in [4].

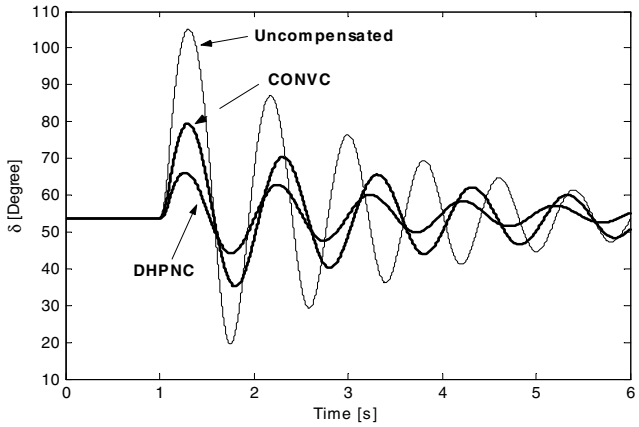

Fig. 19. A 100 ms three phase short circuit test: δ[°].

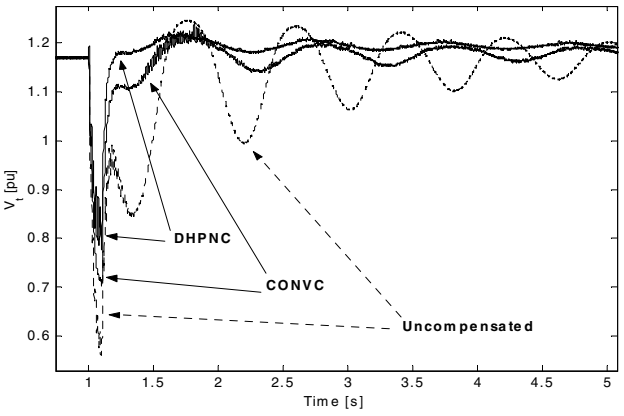

Fig. 20. A 100 ms three phase short circuit test: V_t [pu].

C. Series Capacitive Reactance Compensator (SCRC) and its External and Internal Control

For the series capacitive reactance compensator (SCRC) FACTS device, Ooi *et al.* [22], [23] first proposed making use of a stand-alone inverter both to maintain dc capacitor voltage of the inverter and to ensure the series reactance condition at

the inverter's ac terminals. Rigby and Harley [24] extended the original work proposed by Ooi *et al*. into a working laboratory prototype of a series capacitive reactance compensator (SCRC), and improving the performance of the original SCRC scheme by modifying the voltage regulator structure. Based on this work, they also reported [25] on the analysis of a power oscillation damping scheme by applying an *external linear-controller* with the aid of properly designed supplementary controls [26] to the SCRC, and they also considered the impact of the SCRC's own internal dynamics on the performance of an external damping controller. It is important to note that the study of the *external control* (called secondary or functional operation control [19]) for the FACTS device makes it possible to progress further towards hierarchical control and possible global dynamic optimization in large-scale power networks.

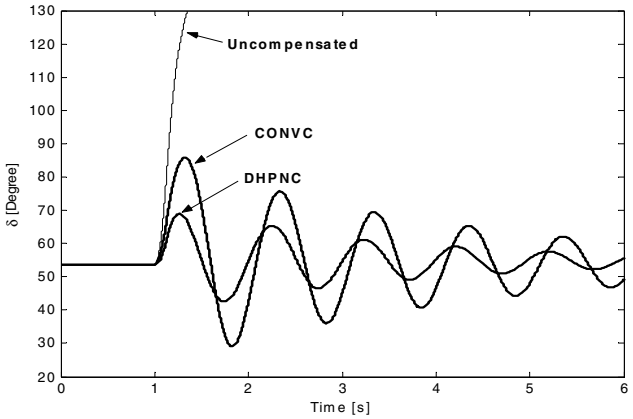

Fig. 21. A 120 ms three phase short circuit test: δ[°].

The theory and operation of the SCRC as well as its conventional external linear-controller (CONVEC) are described in [25] and briefly described by the authors in [5].

The details of the design of a new external optimal neuro-controller (EC) for the SCRC using the dual heuristic programming (DHP) optimization algorithm [2], [4] is proposed as an alternative to the CONVEC in order to improve the damping of low frequency active power oscillations in [5].

The feasibility of the DHPEC is evaluated on the multi-machine power system shown in Fig. 22 equipped with SCRC. This power system model has been used for the study of voltage stability on a practical large-scale power system in [27] and [28]. In Fig. 22, the sending end (in AREA1) has two generators (Gen 1 and Gen 2) transmitting power to the receiving area (AREA 2) through five 500 kV, 200 km long, transmission lines. Gen 1 is given a large inertia so that it functions as the slack bus. However, it is relatively small electrically (5000 MVA) in order to provide only limited voltage support (or reactive power support) for the load area in AREA 2. The parameters of Gen 2 and Gen 3 are identical and given in the Appendix D (Unit *F*18) of [20]. Also, Gen 1 and Gen 2 are equipped with an automatic voltage regulator (AVR)/exciter and a turbine/speed governor system.

The performance of the DHPEC is evaluated by applying a large impulse type disturbance, a 300 ms three phase short circuit to bus 10 (in Fig. 22), at t = 0.5 s. The Gen 2 and Gen 3 are operating with rotor angles of 50.41° and 51.2° with respect to buses 2 and 3 respectively during the pre-fault steady state operating point. The results are shown in Figs. 23 and 24 for the speeds (ω_2 and ω_3) of Gen 2 and Gen 3. They clearly show that the DHPEC still improves damping of low frequency oscillations more effectively, compared to the SCRC (without an external controller).

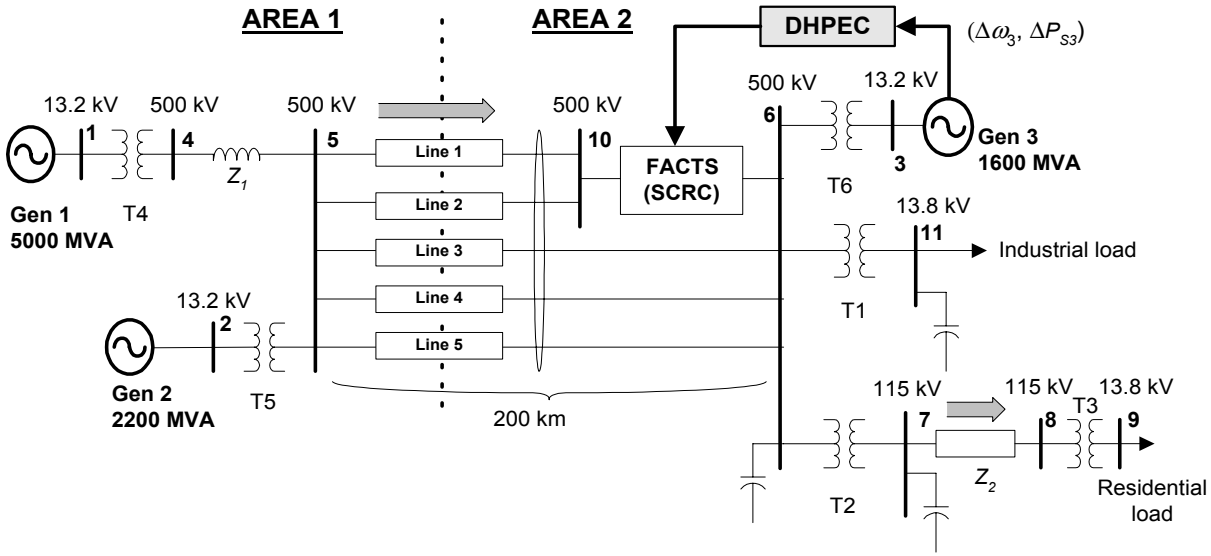

Fig. 22 Large-scale multi-machine power system equipped with SCRC.

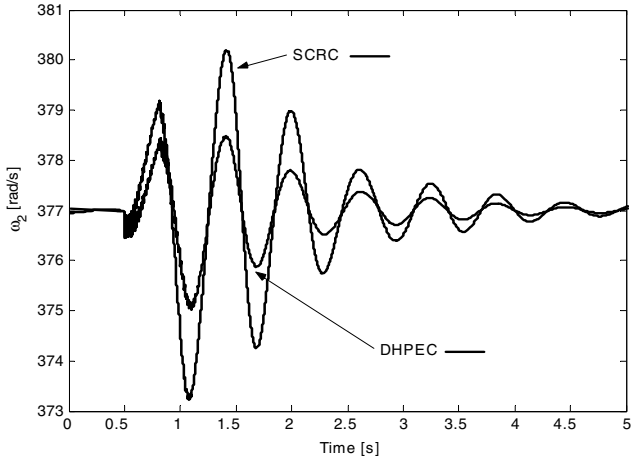

Fig. 23. A 300 ms three phase short circuit test at bus 10: ω_2 [rad/s].

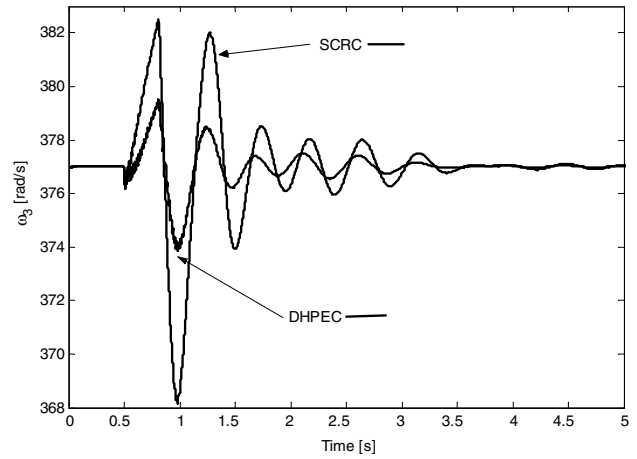

Fig. 24. A 300 ms three phase short circuit test at bus 10: ω_3 [rad/s].

V. Conclusion

This tutorial paper has presented the investigations on the design and implementation of Adaptive Critic based neurocontrollers to replace/augment the conventional PI controllers on generators and FACTS devices, in both single-machine-infinite-bus and multimachine power system. These neurocontrollers exhibit better damping than the conventional controllers. The *Adaptive Critic Design* based neurocontrollers have the great advantage that once trained, their weights/parameters remain fixed and therefore avoid the risk of instability associated with continual online training. The convergence guarantee of the Critic and Action neural networks during offline training was shown in [6, 29]. In addition, the heavy computational load of online training only arises during the offline training phase and therefore makes the online real time implementation cost of the neurocontrollers cheaper. The processing hardware cost is a small fraction of the cost of turbogenerators and therefore this is not a big issue.

The *Adaptive Critic Design* based nonlinear optimal trollers designed in this chapter are all based on approximate models obtained by neuroidentifiers, but nevertheless exhibit superior performance in comparison to the conventional linear controllers which use more extensive linearized models. This benefit of a neuroidentifier agrees with the conclusions on the comparison of using approximate and exact models in adaptive critic designs which was explicitly shown in [7]. All these features are desirable and important for industrial applications which require a neurocontroller technology that is nonlinear, robust and stable.

VI. Appendix

TABLE I
MICRO-ALTERNATOR #1 PARAMETERS

T_{d0}' = 4.50 s	X_d' = 0.205 pu	Rs = 0.006 pu
T_{d0}" = 33 ms	X_d" = 0.164 pu	H = 5.68 s
T_{q0}" = 0.25 s	X_q = 1.98 pu	F = 0
X_d = 2.09 pu	X_q" = 0.213 pu	p = 2 pole pairs

TABLE II
MICRO-ALTERNATOR #2 PARAMETERS

T_{d0}' = 4.50 s	X_d' = 0.205 pu	Rs = 0.006 pu
T_{d0}" = 33 ms	X_d" = 0.164 pu	H = 5.68 s
T_{q0}" = 0.25 s	X_q = 1.98 pu	F = 0
X_d = 2.09 pu	X_q" = 0.213 pu	p = 2 pole pairs

TABLE III
AVR AND EXCITER TIME CONSTANTS

T_{v1}	0.616 s	T_{v5}	0.0235 s
T_{v2}	2.266 s	T_e	0.47 s
T_{v3}	0.189 s	K_{av}	0.003
T_{v4}	0.039 s		

TABLE IV
PSS TIME CONSTANTS AND GAIN

T_W	3 s	T_3	0.045 s
T_1	0.2 s	T_4	0.045 s
T_2	0.2 s	K_{STAB}	33.93

TABLE V
GOVERNOR AND MICRO-TURBINE CONSTANTS

Phase advance compensation, T_{g1}	0.264 s
Phase advance compensation, T_{g2}	0.0264 s
Servo time constant, T_{g3}	0.15 s
Entrained steam delay, T_{g4}	0.594 s
Steam reheat time constant, T_{g5}	2.662 s
pu shaft output ahead of reheater, F	0.322
Gain K_g	0.05

VII. Acknowledgment

The authors acknowledge the University of Kwa-Zulu Natal, Durban, South Africa for allowing the usage of the micro-machines laboratory.

References

[1] G. K. Venayagamoorthy, R. G. Harley, D. C. Wunsch, "Comparison of Heuristic Dynamic Programming and Dual Heuristic Programming Adaptive Critics for Neurocontrol of a Turbogenerator", *IEEE Transactions on Neural Networks*, Volume: 13, Issue: 3, May 2002, Page(s): 764 -773.

[2] G. K. Venayagamoorthy, R. G. Harley, D. C. Wunsch, "Dual Heuristic Programming Excitation Neurocontrol for Generators in a Multimachine Power System", *IEEE Transactions on Industry Applications*, Volume: 39, Issue: 2, March/April 2003.
[3] G. K. Venayagamoorthy, R. G. Harley, D. C. Wunsch, "Implementation of Adaptive Critic Based Neurocontrollers for Turbogenerators for Turbogenerators in a Multimachine Power System", *IEEE Transactions on Neural Networks –Special Issue on Hardware Implementations*, September 2003.
[4] J. W. Park, R. G. Harley, G. K. Venayagamoorthy, "New internal optimal neurocontrol for a series FACTS device in a power transmission line", *Neural Networks*, vol. 16, no. 5-6, July 2003, pp. 881-890.
[5] J. W. Park, R. G. Harley, G. K. Venayagamoorthy, "New External Neuro-Controller for Series Capacitive Reactance Compensator in a Power Network", *IEEE Transactions on Power Systems*, vol. 19, no. 3, August 2004, pp. 1462 - 1472.
[6] D. Prokhorov, L. A. Feldkamp, "Analyzing for Lyapunov Stability with Adaptive Critics", *Proceedings of the International Conference on Systems, Man and Cybernetics*, 1998, Vol. 2, pp. 1658-1161.
[7] T. T. Shannon, G. G. Lendaris, "Qualitative Models for Adaptive Critic Neurocontrol", *Proceedings of the International Joint Conference on Neural Networks*, IJCNN 1999, Washington DC, USA, Vol. 1, pp. 455-460.
[8] Z. Huang, S. N. Balakrishnan, "Robust Adaptive Critic Based Neurocontrollers for Systems with Input Uncertainties", *Proceedings of the International Joint Conference on Neural Networks*, *(IJCNN 2000),* 24 – 27 July, 2000, Como, Italy, Vol. 3, pp. 67-72.
[9] P. J. Werbos, "Approximate Dynamic Programming for Real Time Control and Neural Modelling", in White DA and Sofge DA (Eds.), *Handbook of Intelligent Control,* Van Nostrand Reinhold, New York, 1992, ISBN 0-442-30857-4, pp. 493 - 525.
[10] C. J. Watkins, P. Dayan, "Q-Learning", *Machine Learning*, vol. 8, 1992, pp. 279 – 292.
[11] D. V. Prokhorov, "Adaptive Critic Designs and their Applications", *Ph.D. Thesis*, Texas Tech University, USA, October 1997.
[12] D. V. Prokhorov, D. C. Wunsch, "Adaptive Critic Designs" *IEEE Trans. on Neural Networks*, Vol. 8, No. 5, September 1997, pp. 997 – 1007.
[13] G. K. Venayagamoorthy, R. G. Harley, " A Continually Online Trained Artificial Neural Network Identifier for a Turbogenerator", *Proceedings of IEEE International Electrical Machine and Drives Conference (IEMDC)*, Seattle, USA, May 1999, pp. 404 – 406.
[14] K. S. Narendra, K. Parthasarathy, "Identification and Control of Dynamical Systems using Neural Networks", *IEEE Trans. on Neural Networks*, Vol.1, No. 1, March 1990, pp. 4-27.
[15] D. J. Limebeer, R. G. Harley, S. M. Schuck, "Subsychronous Resonance of the Koeberg Turbogenerators and of a Laboratory Micro-Alternator System", *Trans. of the SA Institute of Electrical Engineers*, November 1979, pp. 278-297.
[16] P. Kundur, M. Klein, G. J. Rogers, M. S. Zywno, "Application of Power System Stabilizers for Enhancement of Overall System Stability", *IEEE Trans. on Power Systems*, Vol. 4, No. 2, May 1989, pp. 614 – 626.
[17] W. K. Ho, C. C. Hang, L. S. Cao, "Tuning of PID Controllers based on Gain and Phase Margin Specifications", *Proceedings of the 12th Triennial World Congress on Automatic Control*, 1993, pp. 199 –202.
[18] G. K. Venayagamoorthy, R. G. Harley, "A Continually Online Trained Neurocontroller for Excitation and Turbine Control of a Turbogenerator", *IEEE Trans. on Energy Conversion*, Vol. 16, No.3, September 2001, pp. 261-269.
[19] N. G. Hingorani, L. Gyugyi, *Understanding FACTS: Concepts and technology of flexible AC transmission systems,* Sponsored by IEEE Power Engineering Society, IEEE Press, 1999, ISBN 0-7803-3455-8.
[20] P. M. Anderson, A. A. Fouad, *Power system control and stability*. New York: IEEE Press, 1994.
[21] T. Makombe, N. Jenkins, "Investigation of a unified power flow controller", *IEE Proc.-Generation, Transmission and Distribution*, 1999, 146(4), 400-408.
[22] X. Wang, S.-Z. Dai, and B. T. Ooi, "A Series Capacitive Reactance Compensator Based on Voltage Source PWM Converter," in *Proc. of IEEE IAS Annual Meeting*, pp. 918-924, 1991.
[23] B. T. Ooi, S.-Z. Dai, and X. Wang, "Solid-State Series Capacitive Reactance Compensators," *IEEE Trans. on Power Delivery*, Vol.7, pp. 914-919, April 1990.
[24] Bruce S. Rigby and R.G. Harley, "An Improved control Scheme for a Series-Capacitive Reactance Compensator Based on a Voltage-Source Inverter," *IEEE Trans. on Industry Applications*, Vol.34, No.2, pp. 355-363, March/April 1998.
[25] Bruce S. Rigby, N.S. Chonco, and R.G. Harley, "Analysis of a Power Oscillation Damping Scheme Using a Voltage-Source Inverter," *IEEE Trans. on Industry Applications*, Vol.38, No.4, pp. 1105-1113, July/August 2002.
[26] F.J. Swift and H.F. Wang, "Application of the controllable series compensator in damping power system oscillations," *IEE Proc.-Gener. Transm. Distrib.*, Vol.143, No.4, pp. 359-364, July 1996.
[27] Carson W. Taylor, "Concepts of Undervoltage Load Shedding for Voltage Stability," *IEEE Trans. on Power Delivery*, Vol.7, No. 2, pp. 480-488, April 1992.
[28] Carson W. Taylor, N. J. Balu, and D. Maratukulam, "Power system control and stability," McGraw-Hill Companies, EPRI Power System Engineering Series, 1993, ISBN 0070631840.
[29] D. V. Prokhorov, D. C. Wunsch, "Convergence of Critic-Based Training", *Proceedings of the IEEE International Conference on Systems, Man, and Cybernetics*, Vol. 4, 1997, pp. 3057 – 3060.

Ganesh Kumar Venayagamoorthy (M'97, SM'02) received the B.Eng. (Honors) degree with a first class honors in Electrical and Electronics Engineering from the Abubakar Tafawa Balewa University, Bauchi, Nigeria, and the MScEng and PhD degrees in Electrical Engineering from the University of Natal, Durban, South Africa, in March 1994, April 1999 and February 2002, respectively. He was a Senior Lecturer at the Durban Institute of Technology, South Africa prior to joining the University of Missouri-Rolla (UMR), USA as an Assistant Professor in the Department of Electrical and Computer Engineering in May 2002. He is the Director of the Real-Time Power and Intelligent Systems Laboratory at UMR. His research interests are in computational intelligence, power systems, evolvable hardware and signal processing. Dr. Venayagamoorthy has attracted in excess of $ 1 million in research funding from external sources since joining UMR. He has published over 130 papers in refereed journals and international conferences. Dr. Venayagamoorthy is the 2005 IEEE Industry Application Society (IAS) Outstanding Young Member award recipient, a 2004 NSF CAREER award recipient, the 2004 IEEE St. Louis Section Outstanding Young Engineer, the 2003 International Neural Network Society (INNS) Young Investigator award recipient, a 2001 recipient of the IEEE Computational Intelligence Society (CIS) W. J. Karplus summer research grant and the recipient of five prize papers with the IEEE IAS and IEEE CIS. He is an Associate Editor of the IEEE Transactions on Neural Networks. He is a Senior Member of the South African Institute of Electrical Engineers, a Member of INNS and the American Society for Engineering Education. He is currently the IEEE St. Louis CIS and IAS Chapter Chair, the Chair of the task force on Intelligent Control Systems and the Secretary of the Intelligent Systems subcommittee of IEEE Power Engineering Society.

Ronald G. Harley (M'77-SM'86-F'92) was born in South Africa. He received the BSc.Eng. (cum laude) and MScEng (cum laude) degrees from the University of Pretoria, Pretoria, South Africa, and the Ph.D. degree from London University, London, U.K., in 1960, 1965, and 1969, respectively. In 1970 he was appointed to the Chair of Electrical Machines and Power Systems at the University of Natal in Durban, South Africa. He is currently at the Georgia Institute of Technology, Atlanta, USA. He has co-authored some 350 papers in refereed journals and international conferences. Altogether 9 papers attracted prizes from journals and conferences. Ron is a Fellow of the SAIEE, a Fellow of the IEE, and a Fellow of the IEEE. He is also a Fellow of the Royal Society in South Africa, a Fellow of the University of Natal, and a Founder Member of the Academy of Science in South Africa formed in 1994. He has been elected as a Distinguished Lecturer by the IEEE Industry Applications Society for the years 2000 and 2001. His research interests are in the dynamic and transient behavior of electric machines and power systems, and controlling them by the use of power electronics and modern control algorithms.